

Spectroscopy of Infrared Flares from the Microquasar GRS 1915+105

S.S. Eikenberry^{1,2}, K. Matthews, T.W. Murphy Jr., R.W. Nelson

Department of Physics
California Institute of Technology
Pasadena, CA 91125

E.H. Morgan, R.A. Remillard, M. Muno
Center for Space Research
Massachusetts Institute of Technology
77 Massachusetts Avenue
Cambridge, MA 02139

Received _____; accepted _____

¹Sherman Fairchild Postdoctoral Fellow in Physics

²Current Address: Department of Astronomy, Cornell University, Ithaca, NY 14853

ABSTRACT

We present near-infrared medium-resolution ($R \sim 875$) spectra of the microquasar GRS 1915+105 on 1997 August 13-15 UTC from the Hale 200-inch telescope. The spectra show broad emission lines of He I ($2.058 \mu\text{m}$) and H I ($2.166 \mu\text{m} - \text{Br}\gamma$), consistent with previous work. On August 14 UTC, we took spectra with ~ 6 -minute time resolution during infrared flaring events similar to those reported in Eikenberry et al. (1998a), which appear to reveal plasma ejection from the system. During the flares, the emission line fluxes varied in approximately linear proportionality to the IR continuum flux, implying that the lines are radiatively pumped by the flares. We also detected a weak He II ($2.189 \mu\text{m}$) emission line on August 14 UTC. The nature of the line variability and the presence of the He II feature indicate that the emission lines in GRS 1915+105 arise in an accretion disk around the compact object, rather than in the circumstellar disk of a proposed Oe/Be companion. The radiative line pumping also implies that the flare emission originates from ejecta which have moved out of the accretion disk plane.

Subject headings: infrared: stars – Xrays: stars – black hole physics – stars:
individual: GRS 1915+105

1. Introduction

The microquasar GRS 1915+105 has attracted considerable interest since its discovery as a hard X-ray transient by GRANAT/SIGMA in 1992 (Castro-Tirado et al., 1995), and study has intensified since the discovery of apparently superluminal jets emanating from the system in 1994 (Mirabel and Rodríguez, 1994), which made it the first member of the class of Galactic microquasars. The microquasars offer tremendous potential as closer, smaller, and faster analogs of the quasars that emit bright radio jets. Recently, multiwavelength studies have shown that GRS 1915+105 exhibits episodes of quasi-periodic ($\sim 20 - 30$ minutes) X-ray dips, where the X-ray flux drops by nearly an order of magnitude in a few seconds and then abruptly recovers. Brightness oscillations with similar timescales have also been seen in the radio and infrared (Pooley & Fender, 1997; Fender et al., 1997). Fitting the X-ray spectra during this behavior, Belloni et al. (1997) have shown that the dips are consistent with a scenario where the X-ray-emitting inner portion of an accretion disk *disappears*. Simultaneous X-ray/infrared (IR) observations in August 1997 revealed such X-ray dips with corresponding large amplitude IR flares, consistent with synchrotron emission from ejected plasma bubbles (Eikenberry et al., 1998a - hereafter Paper 1). Given that GRS 1915+105 is known to eject synchrotron-emitting plasma at relativistic speeds (Mirabel and Rodríguez, 1994), this leads to a picture where the inner portion of an accretion disk is being swept up and ejected from the system in the form of relativistic jets (Paper 1). X-ray/IR/radio observations of dips/flares in September 1997 appear to confirm this interpretation (Mirabel et al., 1998). Thus, it seems that the microquasar GRS 1915+105 is giving the first observational clues into the time-dependent interaction responsible for producing relativistic jets from a black hole accretion disk.

Despite these recent successes, we still know very little about the binary system in GRS 1915+105. Infrared spectra of this heavily obscured object ($A_V \sim 27$ mag; Chaty

et al., 1996) have provided more controversy than conclusion. Castro-Tirado et al. (1996) observed variable, broad He I and H I emission lines from GRS 1915+105. Based on the apparent signature of a weak He II emission line and the IR colors of the system (assuming $A_V \sim 18 - 24$ mag), they argued that the lines arise in an accretion disk around the compact object and that GRS 1915+105 most likely has a low-mass companion star. Mirabel et al. (1997), on the other hand, found that the IR spectra and colors of GRS 1915+105 (assuming $A_V \sim 27$ mag) closely resemble those of many Oe/Be X-ray binaries, where the broad emission lines arise in the circumstellar disk of the high-mass companion star. They failed to detect the He II line, whose presence would argue against an Oe/Be companion since such stars do not emit significant quantities of the 54 eV photons required to doubly ionize helium.

In this paper, we present a spectroscopic study of GRS 1915+105 during the same nights as the photometry presented in Paper 1, when the object exhibited both jet-producing and non-jet-producing behaviors. The results provide constraints for the origin of the IR emission lines, the nature of the mass-donor companion in the binary system, and the origin of the infrared flares accompanying the X-ray dips.

2. Observations and Data Reduction

We obtained infrared spectra of GRS 1915+105 using the HNA longslit grating spectrometer (Larkin et al., 1996) in conjunction with a 256×256 HgCdTe array camera on the Hale 200-inch Telescope. Conditions were photometric on all three nights, and seeing was $\sim 0.5 - 0.8$ arcsec. We tilted the spectrometer grating in order to include the wavelengths of the known emission lines of He I, He II, and H I from GRS 1915+105. The wavelength coverage was $\sim 0.12\mu\text{m}$, centered near $\sim 2.1\mu\text{m}$, with a spectral resolution of $R \sim 875$. We first took images of the source through an open (10×40 arcsec) and closed

(0.7×40 arcsec) slit with a flat mirror in front of the grating. We then took several 5-minute spectral exposures, displacing the source by 20-arcsec along the slit between exposures. The telescope was accurately positioned during these displacements using an image-motion compensatory autoguider. Repointing of the telescope took typically ~ 1 minute, giving a final time resolution of about 6 minutes for the spectra. We also took spectra of bright G-dwarf stars at the same grating tilts and roughly the same airmasses as GRS 1915+105 in order to calibrate atmospheric absorption features. We also obtained simultaneous, intermittent X-ray observations using the Rossi X-ray Timing Explorer (RXTE); details of these are provided in Paper 1.

For each spectral exposure, we subtracted the next exposure, removing bias and sky offsets. After removing cosmic rays, we corrected the frame for spatial distortions using a previously measured transformation, and corrected for spectral distortions using a quadratic fit to the telluric OH lines in the raw frames. We then divided each frame by a similarly processed G-star spectrum (interpolating over the G-star's weak Br γ absorption feature) and multiplied the result by a blackbody spectral shape corresponding to the G-star's effective temperature to obtain the final spectrum.

Due to the photometric variability of GRS 1915+105 on these nights (Paper 1), absolute calibration of the flux levels in the spectra is difficult. For Aug 13 UTC, imaging photometry showed that the source had a fairly steady flux density level of ~ 5 mJy, and we calibrated the Aug 13 spectra by defining this to be the continuum flux density at $2.2\mu\text{m}$. Similarly, the minimum flux seen on Aug 14 and Aug 15 was ~ 5 mJy (Paper 1), and we used this to define the *minimum* observed continuum flux density at $2.2\mu\text{m}$ on these two nights. Comparison of measured flux levels revealed a repeated throughput variation in both the spectra and the slit images, with the flux levels when the source is on one side of the slit greater than those on the other side. This was due to a misalignment between

the spectrometer slit and the telescope motions used to position the source along the slit. After correcting for this effect, we estimate a $\pm 15\%$ uncertainty in the flux levels due to the systematic uncertainty in the placement of the source on the slit.

3. Results

We present the dereddened, flux-calibrated, summed spectra for each spectrograph grating tilt on each night in Figure 1. All of the spectra exhibit resolved, broad He I ($2.058\mu\text{m}$) and Br γ ($2.1655\mu\text{m}$) emission lines. The longer wavelength spectrum taken on Aug 14 shows a He II ($2.189\mu\text{m}$) emission feature. While the signal-to-noise ratio for this feature is low ($\sim 4\sigma$), its properties (Table 1) closely match those seen by Castro-Tirado et al. (1996).

In addition to examining the summed spectra, we also searched the individual 5-minute exposures for evidence of variability in both the continuum flux densities and line fluxes. We found significant variability in the Aug 14 spectra. Plotting a time series of the IR continuum flux density level along with the X-ray count rate from the RXTE PCA instrument at the same time (Figure 2), we surmise that we observed portions of three infrared flares similar to those observed photometrically on the same night (Paper 1). We present individual 5-minute spectra taken during the first IR flare in Figure 3. The most striking feature in this figure is that the emission lines of He I and H I are stronger in the high-flux spectra and weaker in the low-flux spectra. If this correlation was due to systematic throughput variations (such as those we corrected for above), the line equivalent width would remain constant. However, when we examine the individual equivalent widths, we see that they are *not* constant (at the 99.2% confidence level). Together with the similarities in timescale, peak flux, and repetition period to the flares reported in Paper 1, this confirms that the variations are intrinsic to GRS 1915+105. When we plot the

integrated $\text{Br}\gamma$ line flux versus the continuum level (Figure 4), we see that they have an approximately linear correlation, with a scatter corresponding to the variations in the equivalent width.

4. Discussion

4.1. The origin of the emission lines

As noted above, IR spectra of GRS 1915+105 are key to understanding the nature of the binary system – is it a high-mass or low-mass system? In the former case, the lines originate in the circumstellar disk of an Oe/Be-type companion star, while in the latter case, the lines originate in an accretion disk around the compact object. Since O and B stars do not produce the 54 eV photons required to doubly ionize helium, the appearance of a weak He II line in Figure 2 confirms the accretion disk scenario of Castro-Tirado et al. (1996). While we detect this line with a low signal-to-noise, the fact that Castro-Tirado et al. reported a line with identical properties indicates that this feature is most likely real. The fact that the other emission lines are manifestly time variable (Figures 3,4) may explain why the He II feature was not seen by Mirabel et al. (1997) nor at other epochs by Castro-Tirado et al. We also note the similarity in the line ratios for He I, $\text{Br}\gamma$, and He II in our spectra of GRS 1915+105 and the spectrum of Sco X-1 (Bandyopadhyay et al., 1997), which is known to be a low-mass X-ray binary system where the IR emission lines arise in an accretion disk surrounding the compact object. This similarity confirms that such accretion disks are capable of producing the line characteristics we observe here.

The nature of the emission line variability also seems to support the accretion disk interpretation over the Oe/Be-star interpretation. The approximately linear correlation between the emission line flux and continuum flux density in Figure 4 is a signature of

radiative pumping of the HeI and HI emission lines by the flares. While it might be possible for a flare originating near the compact object to pump the line-emitting region of a companion star’s circumstellar disk, roughly half of such a disk would be shielded from the flare by the companion star itself. Since the line profile presumably results from the rotation of the disk, the asymmetric illumination of the disk by the line-pumping flare should dramatically change the line profile – the increased flux should originate from only one portion of the disk, causing the line FWHM to decrease by a factor of ~ 2 and the line centroid to shift to the blue or red as the line flux increases. We can see from Figure 3 and the measured line parameters (Table 1) that no such changes in the line profile are evident. In the accretion disk scenario, on the other hand, the flare could uniformly illuminate the line-emitting region of the disk, and no line profile changes would be evident, which is consistent with the observations.

4.2. The nature of the IR flares

In Paper 1, we demonstrated that the IR continuum emission during the flares is probably dominated by synchrotron emission from particles ejected from the system in the form of relativistic jets. Meanwhile, the broadened profiles of the emission lines suggest that they arise in a rotating disk. However, the fact that the emission line flux is proportional to the flare continuum flux density may provide significant insights into the flares themselves. The proportionality suggests some sort of radiative pumping of the lines by the flares, which in turn requires ultraviolet (UV) radiation during the flares in order to ionize the H and He atoms producing the line emission. The required luminosity of ionizing radiation is only $\sim 10^{25}$ W, but if the UV radiation originates in a distinct region from the IR emission lines, this is only the fraction intercepted by the line-emitting region, and thus represents a lower limit to the total UV radiation during the flare.

Another important insight into the IR flares comes from noting the behavior of GRS 1915+105 on 13 Aug, when no IR flares were observed. On this night the Br γ line flux was near the lowest seen ($\sim 3 \times 10^{-17} \text{W m}^{-2}$) while the X-rays were in a high flux state ($L_x \sim 3 \times 10^{32} \text{ W}$). Since these X-rays arise as thermal emission in the inner accretion disk, they will also be accompanied by thermal UV radiation. Thus, the presence of a large amount of ionizing radiation in the system is not sufficient to produce a high emission-line flux. This leads to two key questions: (1) Why doesn't the high X-ray (and presumably UV) flux on 13 Aug pump the IR emission lines? (2) How does the presence of flaring enable the pumping of the IR emission lines?

Regarding the first question, as noted above both the X-ray and IR line-emitting regions lie in the accretion disk plane. For a thin disk, essentially no ionizing radiation will reach the IR emission region *through* the disk. Therefore, unless the disk is strongly curved, the IR line region will have a small solid angle as seen from the inner disk, and will intercept little ionizing radiation. Thus, for a “standard” thin accretion disk, we may expect that the inner disk radiation will not significantly pump IR emission lines, which is consistent with the observations on 13 Aug 1997. This leads to a possible answer to the second question: the flares can enable the pumping of the IR emission lines due to the presence of ejecta. In Paper 1, we showed that the IR flares are consistent with synchrotron emission from particles ejected from the system. If so, then as the particles move out of the disk plane, the IR line-emitting region subtends a rapidly increasing solid angle as seen from the ejecta. Therefore, we suggest that IR emission line variability may be due to radiative pumping by ionizing radiation from the ejecta. The ionizing radiation could be a UV tail to the synchrotron emission from the ejected plasma which generates the IR flare.

5. Conclusions

We have presented near-IR medium-resolution ($R \sim 875$) spectra of the Galactic microquasar GRS 1915+105 taken using the HNA spectrometer on the Hale 200-inch telescope on 1997 Aug 13-15 UTC. The spectra reveal broad emission lines of He I, H I ($\text{Br}\gamma$), and He II. The presence of the He II line and the relative constancy of the $\text{Br}\gamma$ line profile as its flux changes by factors of ~ 5 imply that the lines originate in an accretion disk around the compact object, as suggested by Castro-Tirado et al. (1996), rather than in the circumstellar disk of an Oe/Be companion star, as suggested by Mirabel et al. (1997). The emission line flux is approximately linearly proportional to the continuum flux during several infrared flares, implying that the flares are associated with radiative pumping of the line emission. This, together with the low line flux seen during a high X-ray flux state on 13 Aug 1997, implies that the IR flares signify the ejection of material out of the accretion disk plane, in agreement with the results in Paper 1.

The authors wish to thank G. Neugebauer for useful discussions of these observations, and T. Prince for access to the computers used to reduce this data. SE acknowledges the support of a Sherman Fairchild Postdoctoral Fellowship in Physics. Infrared astronomy at Caltech is supported by grants from NASA and the National Science Foundation.

REFERENCES

- Bandyopadhyay, R., Shahbaz, T., Charles, P.A., van Kerkwijk, M.H., Naylor, T. 1997, MNRAS, 285, 718
- Belloni, T., Mendez, M., King, A.R., van der Klijns, M., van Paradijs, J. 1997, ApJ, 488, L109
- Castro-Tirado, A.J., et al., 1995, ApJS, 92, 469
- Castro-Tirado, A.J., Geballe, T.R., Lund, N. 1996, ApJ, 461, L99
- Chaty, S., Mirabel, I.F., Duc, P.A., Wink, J.E., Rodríguez, L.F. 1996, A & A, 310 825
- Eikenberry, S.S., Matthews, K., Morgan, E.H., Remillard, R.A., Nelson, R.W. 1998a, ApJ, 494, L61 (Paper 1)
- Eikenberry, S.S., Matthews, K., Morgan, E.H., Remillard, R.A., Nelson, R.W. 1998b, in preparation.
- Fender, R.P. et al. 1997, MNRAS, 290, L65
- Larkin, J.E., Knop, R.A., Lin, S., Matthews, K., Soifer, B.T. 1996, PASP 108, 211
- Mirabel, I.F. and Rodríguez, L.F. 1994, Nature, 371, 46
- Mirabel, I.F., Bandyopadhyay, R., Charles, P.A., Shahbaz, T., Rodríguez, L.F. 1997, ApJ, 477, L45
- Mirabel, I.F., Dhawan, V., Chaty, S., Rodríguez, L.F., Marti, J., Robinson, C.R., Swank, J., Geballe, T. 1998, A & A, 330, L9
- Murphy, T.W. Jr., Eikenberry, S.S., et al., in preparation
- Orosz, J.A. and Bailyn, C.D. 1997, ApJ, 477, 876
- Pooley, G. & Fender, R.P. 1997, MNRAS, 292, 925

Table 1. Properties of emission lines observed from GRS 1915+105. In determining the line FWHM, we have subtracted the spectrograph resolution (~ 340 km/s) in quadrature from the actual observed line width. The centroid uncertainty is for the last digit. The first 4 rows are for Br γ lines in the summed spectra, the fifth row is for the HeII line in the summed spectrum of 14 Aug, and the remaining rows are for the Br γ lines in the individual 300-second exposures on 14 Aug. We estimate the uncertainties in the line properties by first estimating the $\pm 1\sigma$ noise in each pixel as the rms residual for a low-order polynomial fit to a section of the continuum spectrum. Next, we add to each pixel a random number drawn from a normal distribution with that 1σ width, and re-measure the line properties for this simulated spectrum. Finally, we repeat this process 1000 times, and take the standard deviation of the resulting line properties as the $\pm 1\sigma$ uncertainty,

Date	UTC Time (hours)	Flux (10^{-18} W m $^{-2}$)	Centroid (μ m)	FWHM (km/s)
13 Aug	9.0-9.6	28 \pm 6	2.1644 \pm 8	360 \pm 190
14 Aug	8.4-8.9	66 \pm 12	2.1651 \pm 4	230 \pm 60
14 Aug	8.9-9.6	65 \pm 11	2.1650 \pm 4	330 \pm 80
15 Aug	8.7-9.2	28 \pm 7	2.1640 \pm 20	230 \pm 300
14 Aug	8.9-9.6	15 \pm 5	2.189 \pm 12	440 \pm 210
14 Aug (A)	8.4-8.5	30 \pm 11	2.1663 \pm 7	640 \pm 220
14 Aug (B)	8.5-8.6	115 \pm 23	2.1649 \pm 7	230 \pm 110
14 Aug (C)	8.6-8.7	64 \pm 15	2.1650 \pm 6	200 \pm 200
14 Aug (D)	8.7-8.8	97 \pm 25	2.1653 \pm 4	360 \pm 220
14 Aug (E)	8.8-8.9	25 \pm 10	2.1654 \pm 17	200 \pm 200
14 Aug	8.9-9.0	50 \pm 12	2.1643 \pm 9	330 \pm 120
14 Aug	9.0-9.1	134 \pm 28	2.1655 \pm 4	200 \pm 200

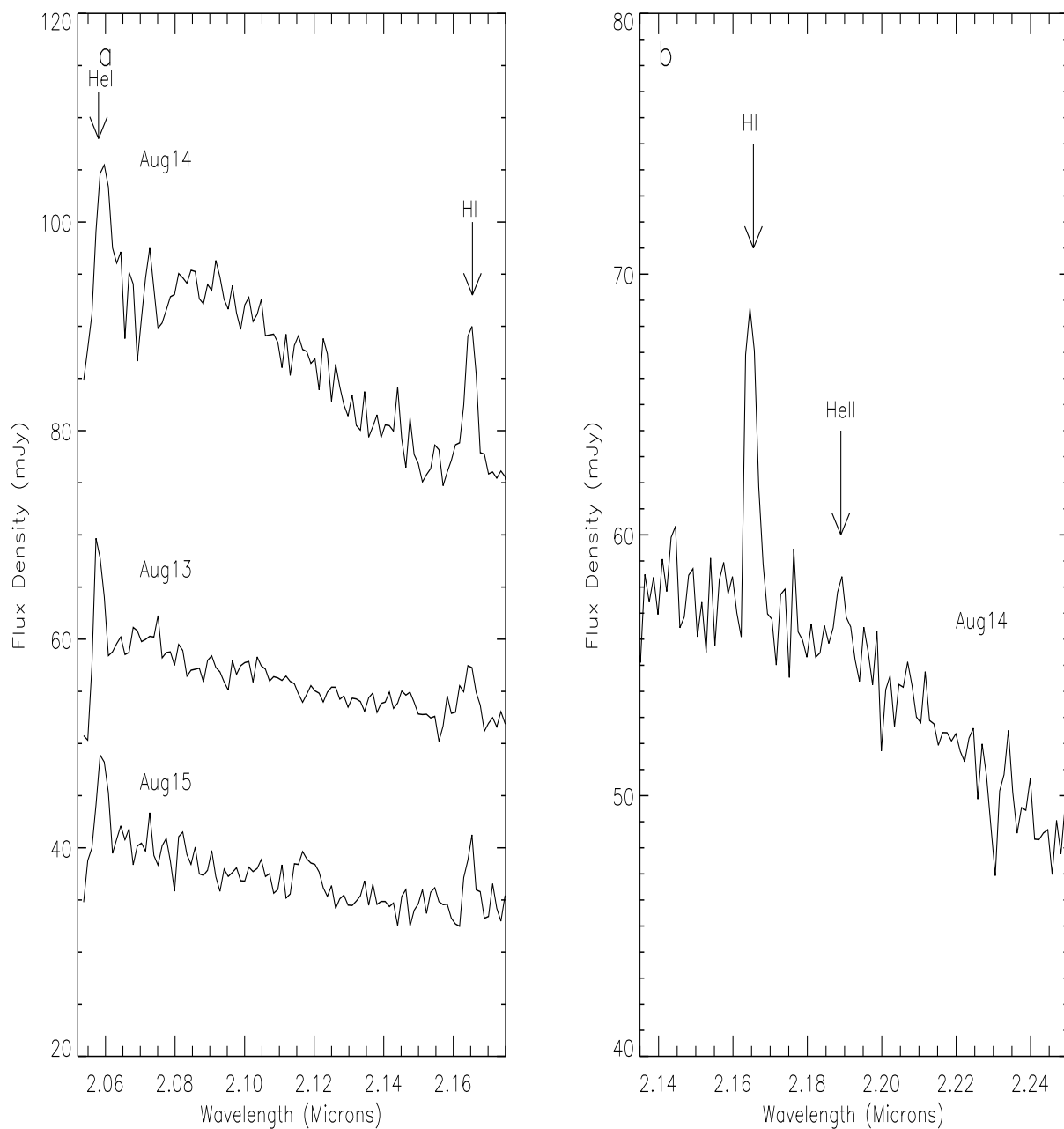


Fig. 1.— Summed infrared spectra from GRS 1915+105 over two wavelength intervals. In (a), the Aug 13 spectrum has been offset by +15 mJy, for the sake of clarity. Arrows indicate emission lines of He I ($2.058\mu\text{m}$), HI ($\text{Br}\gamma = 2.166\mu\text{m}$), and He II ($2.189\mu\text{m}$). Unfortunately, the He I line, while obviously present, is “falling off” the detector array, making quantitative measurements of its properties difficult. All spectra have been dereddened assuming $A_V = 27$ mag ($A_K = 3.0$ mag)

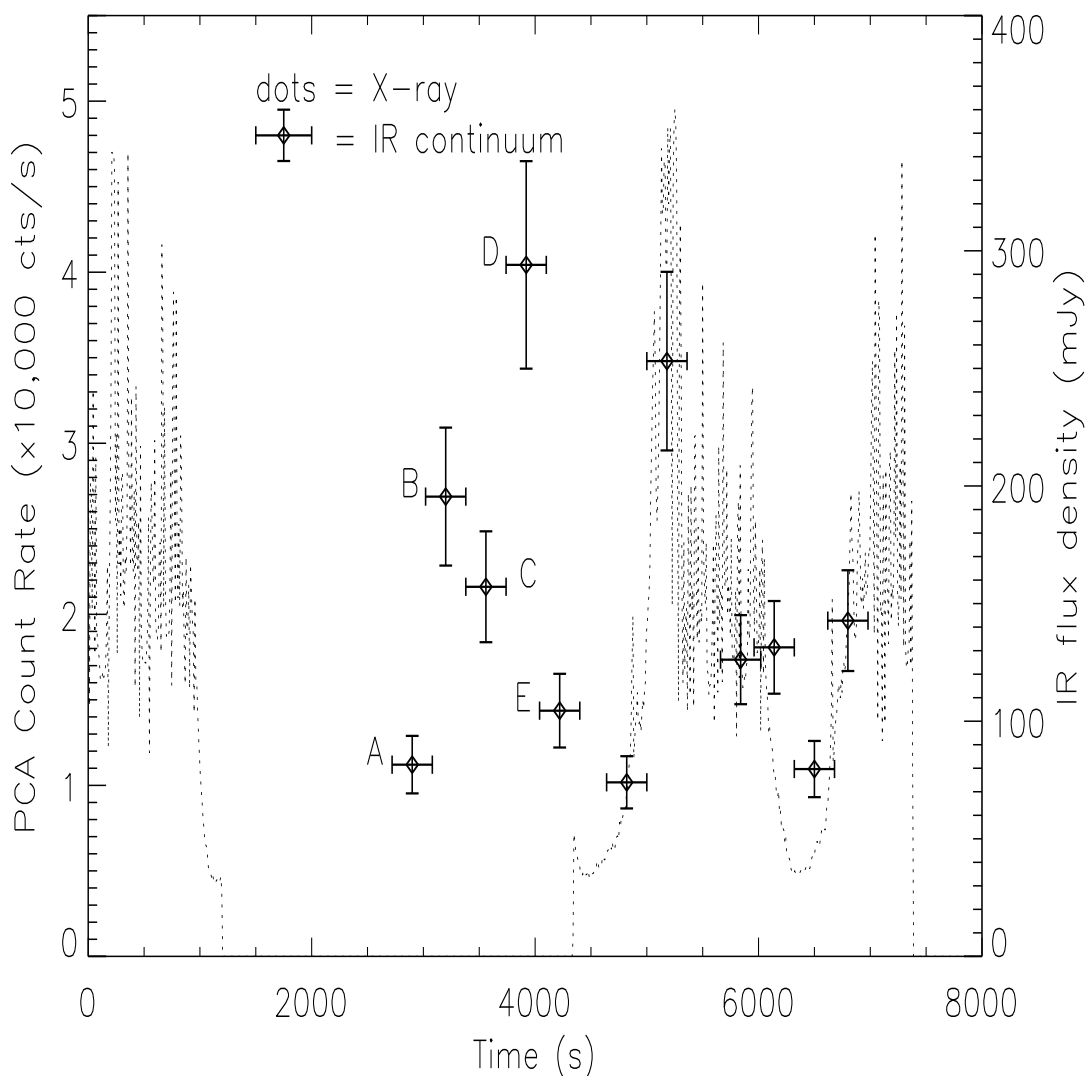


Fig. 2.— IR continuum flux density at $2.16\mu\text{m}$ and RXTE PCA X-ray count rate versus time on 1997 Aug 14 UTC. The X-ray count rates have been averaged over 8-second intervals, and the gaps between $\sim 1200 - 4300$ s and after ~ 7300 s are due to Earth occultations. The IR flux densities have been dereddened assuming $A_V = 27$ mag ($A_K = 3.0$ mag). Error bars indicate the $\pm 1\sigma$ uncertainties. The origin of the time axis corresponds to 7:36 UT.

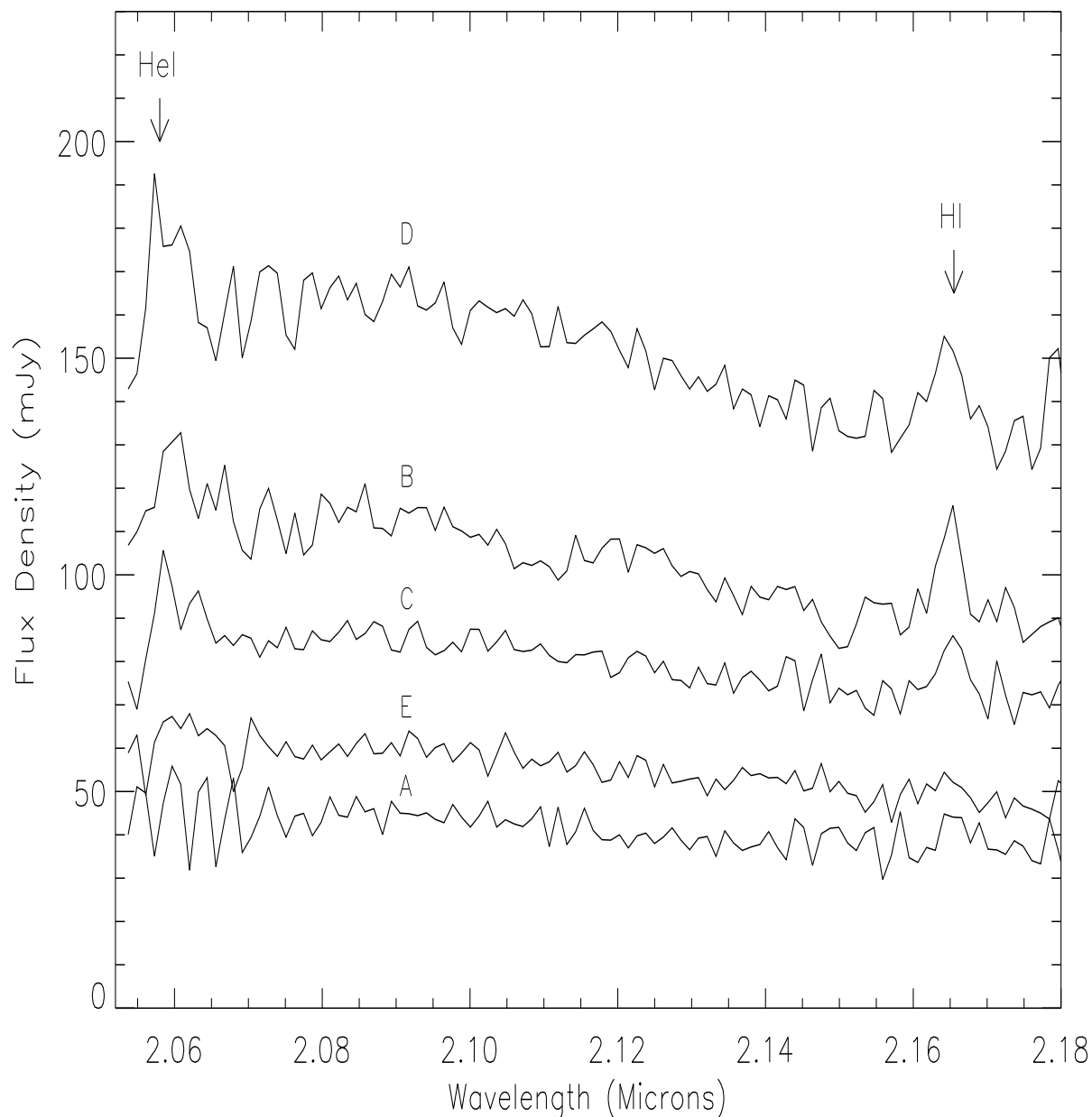


Fig. 3.— Individual 5-minute spectral exposures during an IR flare on 1997 Aug 14 UTC. The time order of the spectra is A,B,C,D,E (see Figure 2). Note that the overall offset of B above C is consistent with 0 within the photometric uncertainties. Arrows indicate emission lines of He I ($2.058\mu\text{m}$) and HI ($\text{Br}\gamma = 2.166\mu\text{m}$). Note that the emission line strength appears to be correlated with continuum flux level. All spectra have been dereddened assuming $A_V = 27$ mag ($A_K = 3.0$ mag).

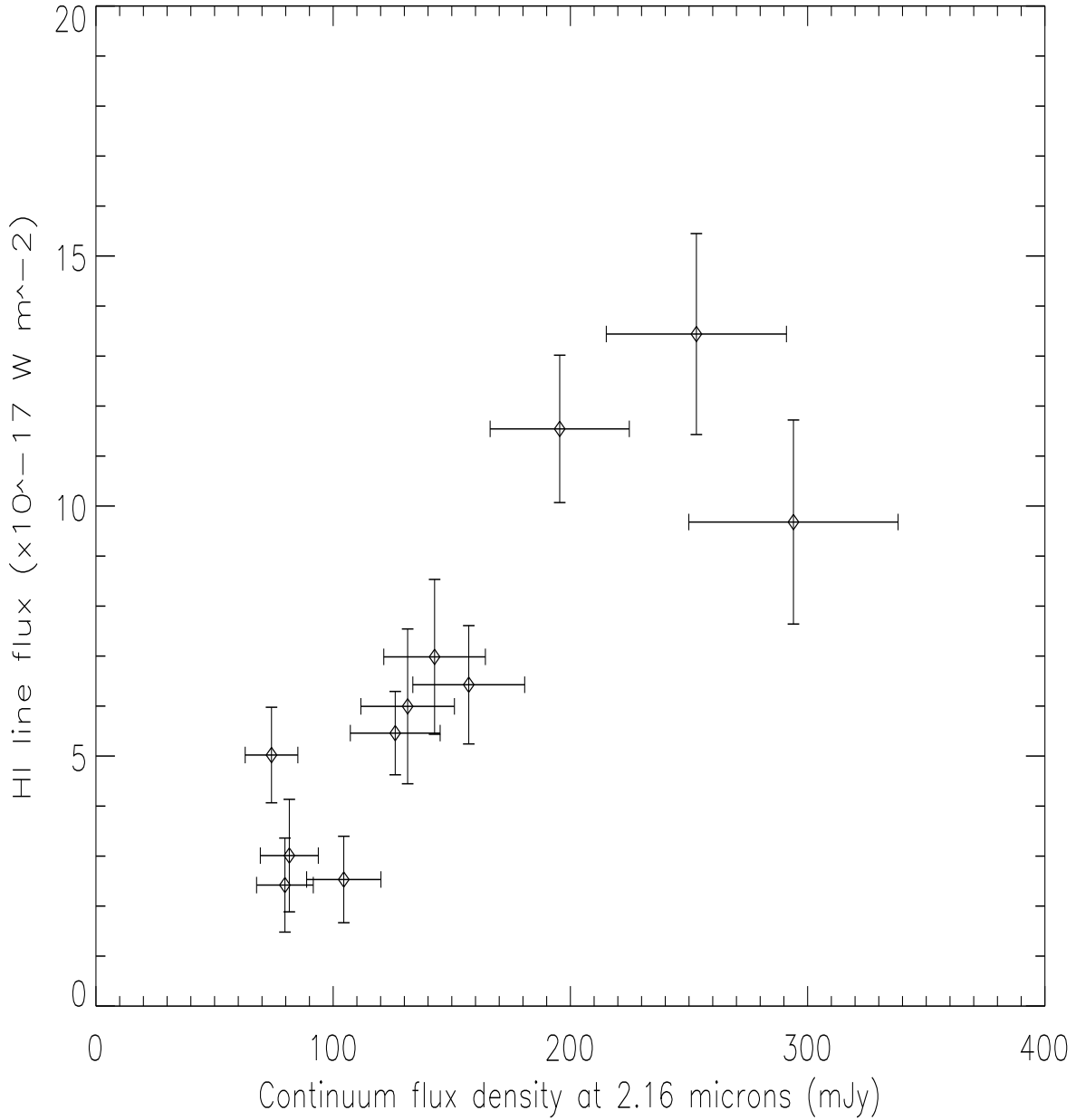


Fig. 4.— HI ($\text{Br}\gamma = 2.166\mu\text{m}$) integrated line flux versus $2.16\mu\text{m}$ continuum flux density for spectra taken during IR flares on 1997 Aug 14 UTC. Error bars indicate the $\pm 1\sigma$ uncertainties. Note the approximately linear dependence of the line flux on the continuum flux density. All spectra have been dereddened assuming $A_V = 27 \text{ mag}$ ($A_K = 3.0 \text{ mag}$).